Experimental and numerical analysis of concrete slabs reinforced with rebar and recycled steel fibers from waste car tyres

Frančić Smrkić, Marina; Damjanović, Domagoj; Baričević, Ana; Uroš, Mario

Experimental and numerical analysis of concrete slabs reinforced with rebar and recycled steel fibers from waste car tyres

Article *in* Structural Concrete · December 2022

DOI: 10.1002/suco.202200640

CITATIONS
2

READS
180

4 authors:

Marina Frančić Smrkić
University of Zagreb
14 PUBLICATIONS **71** CITATIONS
SEE PROFILE

Domagoj Damjanović
University of Zagreb
74 PUBLICATIONS **469** CITATIONS
SEE PROFILE

Ana Baricevic
University of Zagreb Faculty of Civil Engineering
69 PUBLICATIONS **702** CITATIONS
SEE PROFILE

Mario Uros
Civil Engineering Institute Macedonia
49 PUBLICATIONS **367** CITATIONS
SEE PROFILE

Received: 7 July 2022 | Revised: 6 October 2022 | Accepted: 4 December 2022

DOI: 10.1002/suco.202200640

ARTICLE

fib CEB-FIP WILEY

Experimental and numerical analysis of concrete slabs reinforced with rebar and recycled steel fibers from waste car tyres

Marina Frančić Smrkić[1] | **Domagoj Damjanović**[1] | **Ana Baričević**[2] | **Mario Uroš**[1]

[1]Department of Engineering Mechanics, Faculty of Civil Engineering, University of Zagreb, Zagreb, Croatia

[2]Department of Materials, Faculty of Civil Engineering, University of Zagreb, Zagreb, Croatia

Correspondence
Marina Frančić Smrkić, University of Zagreb, Faculty of Civil Engineering, Fra Andrije Kačića Miošića 26, 10000 Zagreb, Croatia.
Email: marina.francic.smrkic@grad.unizg.hr

Funding information
7th Framework Programme of the European Community "Innovative Use of All Tyre Components in Concrete", Grant/Award Number: 603722

Abstract

In light of various initiatives taken around the world to convert waste materials into new products, the objective of this paper is to promote the use of steel fibers from recycled car tyres in the concrete industry. Hybrid steel fiber reinforced concrete (HSFRC) is a material that combines two or more types of steel fibers, in this case: manufactured steel fibers and recycled steel fibers from waste car tyres in equal proportions. The main objective of the presented research was to investigate the possible application of HSFRC in structural elements with conventional reinforcing bars in order to improve the flexural behavior and to investigate the possibility of partially replacing the conventional reinforcement with steel fibers in terms of service performance. For this purpose, eight slab specimens with different reinforcement ratios were subjected to a four-point bending test to measure displacements, strength, and crack widths. The addition of a hybrid fiber mix to a conventionally reinforced concrete slab significantly reduced crack widths by up to 53%. The addition of fibers compensated for a conventional reinforcement reduction of 20% by reducing crack widths by up to 38%. It was observed that slightly more cracks opened with smaller widths and at smaller distances from each other in these slab types than in the conventionally reinforced reference slabs. Slabs with hybrid fiber mix and 44% reinforcement reduction showed no improvement in crack control compared to the conventionally reinforced concrete reference slabs. Using numerical models in ABAQUS simulating the flexural test on notched prismatic specimens, a calibration of the material models of plain concrete, and HSFRC was performed based on the test results. These validated material models were used for numerical modeling of slabs. The results of the analyses compared with the experimental results showed good agreement and

Discussion on this paper must be submitted within two months of the print publication. The discussion will then be published in print, along with the authors' closure, if any, approximately nine months after the print publication.

confirmed the ability of the proposed material model of HSFRC to predict the flexural behavior of slabs with conventional reinforcement.

KEYWORDS

concrete slabs, crack width, finite element analysis, recycled steel fibers, seviceability limit state, steel fiber reinforced concrete

1 | INTRODUCTION

Waste management is one of the greatest challenges facing developing countries. In modern waste management systems, recycling and reuse of waste is given preference over disposal. The proper disposal of waste tyres presents a particular challenge, as they can be the cause of environmental disasters such as long-term fires. Fires that develop in tyre landfills are usually wildfires that are difficult to control and suppress, leading to significant development of toxic smoke.[1] Many of the current regulations governing the tyre disposal process prioritize reuse and recycling over disposal, with the goal of generating either materials or energy. Considering the various initiatives taken around the world to convert waste materials into new products, the objective of this paper is to promote the use of steel fibers from recycled car tyres in the concrete industry.

Steel fiber reinforced concrete (SFRC) can be used to improve the performance of concrete structures by controlling cracks, replacing minimal shear reinforcement, or increasing flexural strength. Wider application of manufactured steel fibers is limited to a small number of structures mainly because of their high price. Therefore, many researchers are focusing on finding alternative types of fibers, such as steel fibers obtained as a by-product from the mechanical recycling of car tyres.[2–6] These recycled fibers are cheaper than manufactured fibers and their use helps to solve the environmental problem of waste tyre disposal. In terms of sustainability, life cycle assessment studies show that the production of recycled steel fibers requires only 5% of the energy compared to manufactured steel fibers.[7] Previous studies have shown that recycled steel fibers can replace manufactured steel fibers, although not completely, to a certain extent.[1,8] Therefore, the idea of combining manufactured and recycled steel fibers to produce hybrid steel fiber reinforced concrete (HSFRC) was developed. Previous studies[1,8,9] have shown that HSFRC can be an alternative to standard SFRC from a technical, economic and environmental point of view.

Reinforced concrete elements are designed to meet both ultimate and serviceability limit state criteria. The addition of fibers to concrete in low to moderate volume proportions (0.4%–1% according to Zollo[10]) increases ductility and fracture energy, but has no significant effect on tensile strength. Therefore, conventional reinforcement cannot be entirely replaced by fibers concerning the ultimate limit state, but better cracking behavior can be achieved by the combined action of reinforcing bars and fibers.[11] Control of cracking at the serviceability limit state is one of the main reasons for using SFRC. When the design requires more steel than is necessary to meet the strength requirements, which is often the case for bridge slabs, the use of SFRC may be a suitable alternative. A number of experimental studies have been carried out on the flexural behavior of structural elements with SFRC and longitudinal reinforcing bars, but only a limited number provide data on the effects of fibers on serviceability, such as crack width and reinforcement strains.[12–14]

The objective of this study was to investigate the potential application of HSFRC in structural elements with conventional reinforcement, and to promote the use of recycled steel fibers as an effective and sustainable way of dealing with cracking. Another objective was to investigate the possibility of partially replacing conventional reinforcement with recycled steel fibers in terms of service performance. Therefore, a total of eight HSFRC and plain concrete slabs with different conventional reinforcement ratios were subjected to a four-point bending test to measure displacements and crack widths.

In modern research in civil engineering, finite element analysis (FEA) is essential to gain insight into structural behavior. Nonlinear FEA can reveal crack initiation and propagation, deflections and failure mechanisms. In the numerical analysis of concrete elements, the fundamental challenge is to model the material itself due to its complex properties. The addition of steel fibers magnifies this problem. Computer programmes for numerical analysis using the finite element method offer a choice of embedded material models, but also allow the creation of customized material models. Experimental values of mechanical properties obtained from laboratory tests can be used to create a characteristic material model of concrete under ideal conditions. The main challenge is the tensile testing of concrete, which is difficult to perform and is usually replaced by flexural tests, which are much easier but do not provide direct results. Therefore, using numerical models in ABAQUS to simulate the flexural test on notched prismatic specimens, a calibration of the material models of plain concrete and HSFRC was

performed based on the test results. These validated material models were used for numerical modeling of slabs and the results were compared with the experimental values in terms of deflections, strength, and crack patterns. The aim of this paper is to present a calibrated material model for HSFRC to describe and analyze the bending behavior on real-scale specimens.

2 | MATERIALS AND METHODS

2.1 | Materials

The concrete was made with Portland cement type CEM II/A-M (S-V) 42.5 N, river aggregate with a maximum grain size of 16 mm (0/4 , 4/8 and 8/16 mm), and a polycarboxyl ether superplasticizer. The grading curves of the aggregates used in this study are shown in Figure 1.

Steel fibers (MF) of the type HE 55/35, manufactured by ArcelorMittal, were used as reference fibers. These fibers are straight with hooked ends and their properties are listed in Table 1. Recycled tyre steel fibers (RTSF) of type R-AFT 01/25 were provided by Twincon Ltd. These fibers have an irregular shape and vary in length and diameter. The average geometrical and mechanical properties of the RTSF used are listed in Table 1. Figure 2 shows both types of fibers. Grade B500B steel was used for the reinforcement.

2.2 | Mix design

The experimental programme included two concrete mixes: the reference mix of plain concrete (labeled PC) and a HSFRC mix (labeled HSFRC) reinforced with both manufactured steel fibers and recycled steel fibers. Two

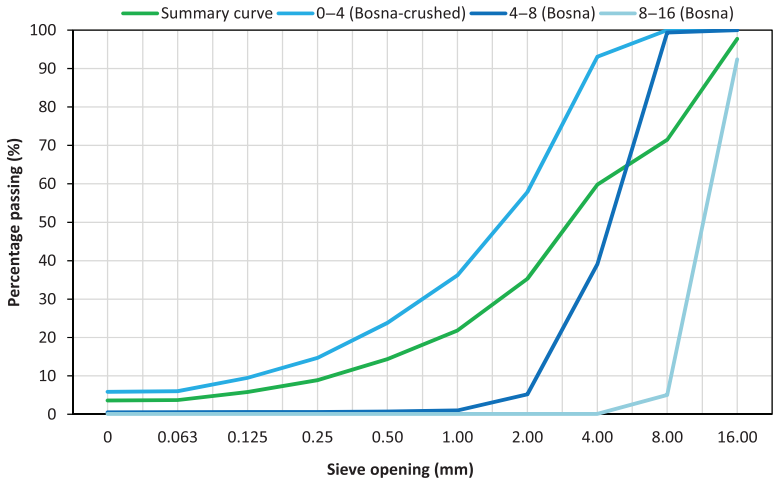

FIGURE 1 Grading curves of aggregates

TABLE 1 Geometrical and mechanical properties of manufactured fibers and recycled steel fibers

Fiber ID	Geometrical shape	Length L (mm)	Diameter D (mm)	Aspect ratio L/D	Tensile strength (N/mm^2)
MF	Straight with hooked ends	35.0 (+2/−3)	0.55 (±0.04)	64	1200
RTSF	Irregular	20.0 (±2.0)	0.15 (±0.04)	166	2850

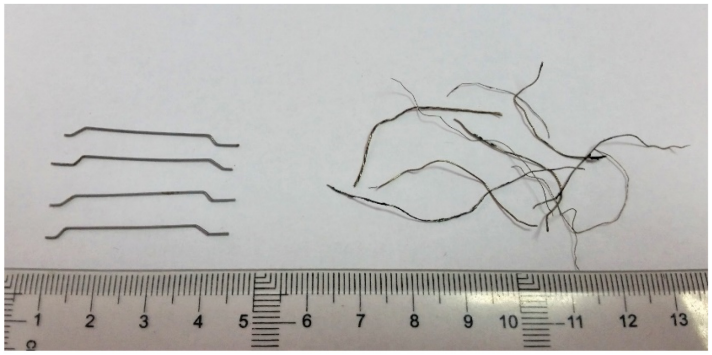

FIGURE 2 Manufactured fibers (left) and recycled tyre steel fibers (right)

concrete mixes were selected based on extensive previous research by the authors,[1,8,9] which confirmed similar post-cracking behavior of the HSFRC mix compared to the SFRC mix with only manufactured steel fibers. In the HSFRC mix, the manufactured and recycled fibers were used in equal proportions. Table 2 shows the concrete mix design and fiber dosage.

All concrete mixes were produced in the precast concrete plant. All components were manually added to the mixer and weighed before the mixing process started. The mixing process was as follows. First, the entire amount of aggregates and half of the mixing water were mixed. Then the cement was added along with the remaining water and superplasticizer. Finally, the fibers were added manually (MF) and with the help of the specially designed rotating drum (RTSF) to prevent the fibers from clumping.

TABLE 2 Mix proportions

Component (kg/m^3)	PC	HSFRC
Aggregate (all sizes)	1808	1794
Cement	370	370
Water	170	170
w/c ratio	0.46	0.46
Superplasticizer	2.22	2.22
Manufactured steel fibers	0	20
Recycled steel fibers	0	20

2.3 | Specimen description

The studies presented here were carried out in two phases: (a) on small-scale specimens, (b) on real-scale specimens.

The material properties were tested on three PC specimens and nine HSFRC specimens. The cubes, cylinders, and prisms were used to determine the compressive strength, modulus of elasticity, splitting tensile strength, and flexural strength. After determining the slump (class S4), the concrete was poured into a hopper for easier handling. The concrete was poured in two layers and each layer was vibrated on a vibrating table for 10–20 s. The specimens were stored under laboratory conditions (temperature 21 ± 3°C) for 24 h until demolding and cured in tanks with water for 28 days.

The real-scale specimens consisted of four types of slab specimens (Table 3 and Figure 3). All specimens had

TABLE 3 Specimen types and labels

Type	Concrete mix	Specimens ID	Reinforcement	Reinforcement ratio (%)	Reinforcement reduction (%)
PC	PC	PC-S1	5Φ12	0.76	–
		PC-S2			
H1	HSFRC	H1-S1	5Φ12	0.76	–
		H1-S2			
H2	HSFRC	H2-S1	4Φ12	0.61	20
		H2-S2			
H3	HSFRC	H3-S1	4Φ10	0.42	44.4
		H3-S2			

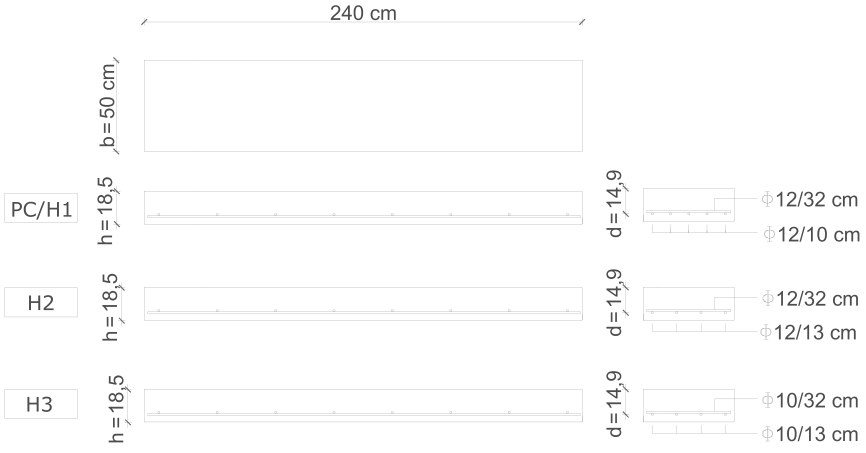

FIGURE 3 Dimensions and reinforcement plan of the specimen types

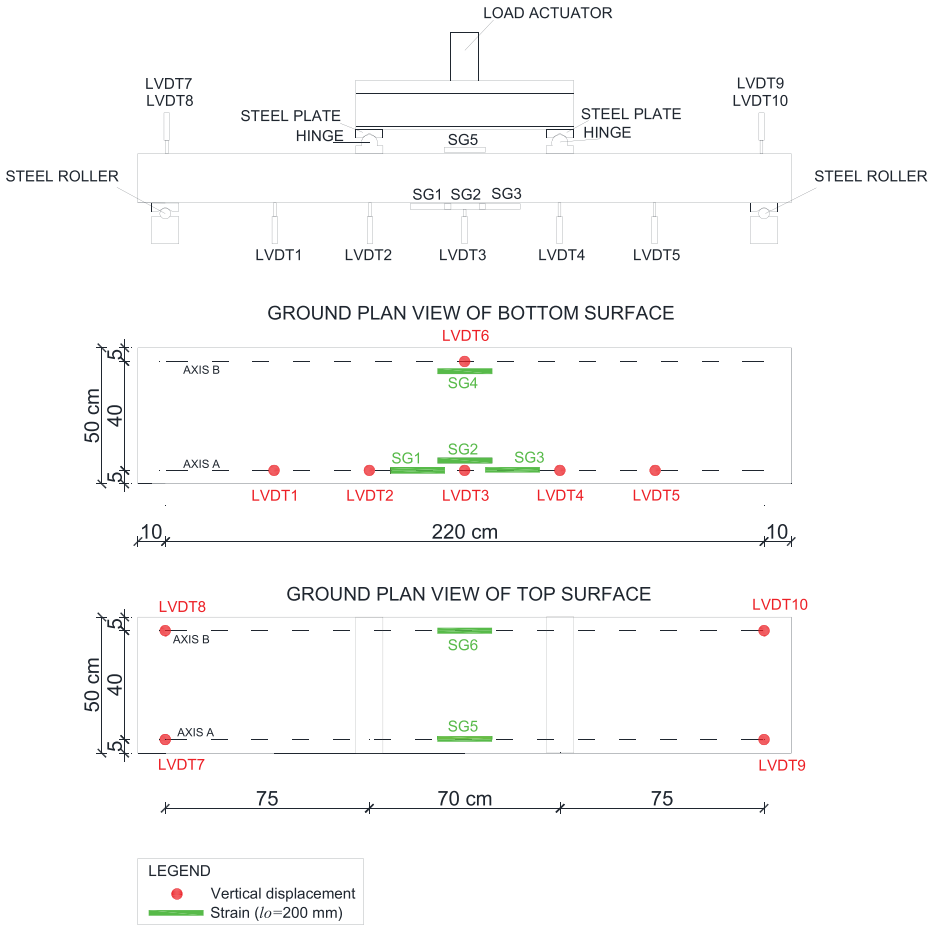

FIGURE 4 Measurement equipment and disposition of measurement points

TABLE 4 Parameters used in FE model

Dilatation angle ψ (°)	Eccentricity ϵ	σ_{b0}/σ_{c0}	K_c	Viscosity parameter	Poisson's ratio
38	0.1	1.16	0.667	0	0.2

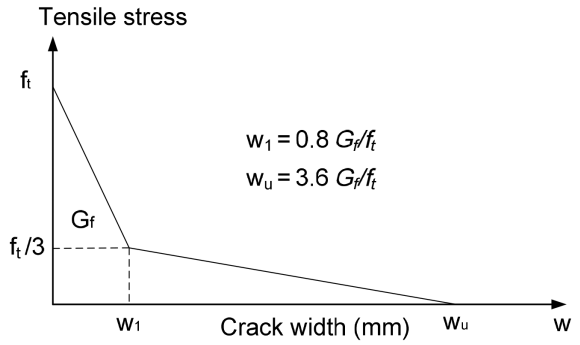

FIGURE 5 Uniaxial tensile stress-crack width relationship for concrete

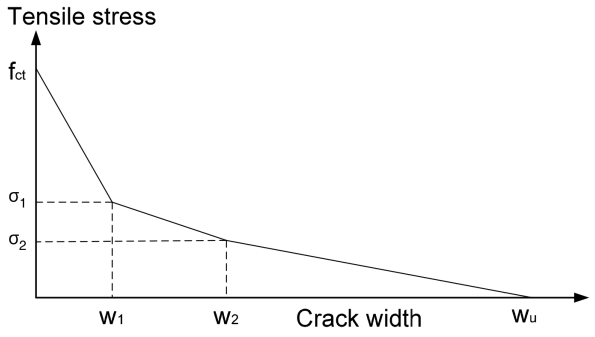

FIGURE 6 Material model for HSFRC

the same dimensions of 240 × 50 × 18.5 cm and represented part of the bridge deck that was adapted for laboratory-scale testing. The concrete cover was 3 cm on the tension side, while the effective depth was 14.9 cm. The reference mix used was PC, with a conventional reinforcement ratio of 0.76%, representing a typical section of a bridge deck. Types H1, H2, and H3 cast in HSFRC had conventional reinforcement ratios of 0.76%, 0.61%, and 0.42%, respectively. Grade B500B reinforcing steel was

	f_{ct} (MPa)	σ_1 (MPa)	σ_2 (MPa)	w_1 (mm)	w_2 (mm)	w_u (mm)
PC	3.58	1.1	–	0.018	–	0.125
HSFRC	6.13	2.5	1.8	0.010	0.35	2

TABLE 5 Properties of material models

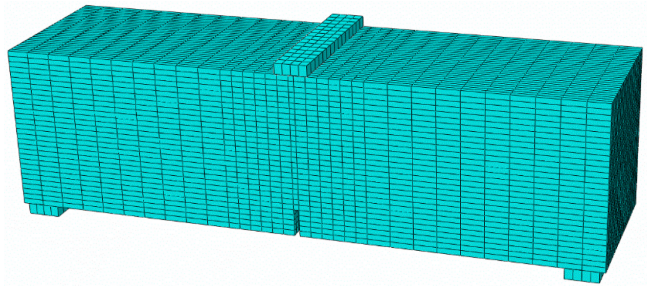

FIGURE 7 Geometry and mesh of notched prismatic specimen

used. The specimens were produced in a steel formwork directly on a vibrating table and vibrated for about 60 s. After casting, they were covered with plastic sheets to reduce the sudden evaporation of water and to maintain the temperature. After 4 days, the specimens were demolded and transported to the testing laboratory. The specimens were tested when they were at least 3 months old.

2.4 | Test set-up

The compressive strength was tested after 28 days on 150 mm cubes, as well as the average modulus of elasticity and the tensile splitting strength (both measured on 150 × 300 mm cylinders) according to EN 12390.[15–17] The flexural tensile strength was determined on 150 × 150 × 600 mm prismatic specimens with a 25 mm deep notch in the center.[18]

The properties of reinforcing steel were determined according to EN ISO 15630-1:2010[19] and EN ISO 6892-1:2009[20] on three specimens for each diameter type (10 and 12 mm).

A total of eight real-scale specimens were tested at 3 months of age. The specimens were simply supported with a span of 220 cm on steel rollers with a radius of 40 mm and subjected to four-point bending. The specimens were loaded under displacement control at a rate of 3 mm/min in 25 kN increments. The load was applied by a servo-hydraulic actuator with a capacity of 600 kN. During the bending tests, 10 linear variable differential transformers (LVDTs) were attached to the top and bottom of the specimens to measure the vertical displacements, LVDT1-LVDT10, Figure 4. Strains were measured at the compression (SG5, SG6) and tension (SG1-SG4) surfaces of the specimens using inductive sensors with a gauge length of 200 mm, Figure 4. After the initial cracking, inductive sensors were used to monitor the crack widths. Since more than one crack occurred in the measurement area of the sensor, the crack widths were also measured with a digital microscope (0.02 mm accuracy).

3 | NUMERICAL RESEARCH

In this study, the FE analysis package ABAQUS was used to perform nonlinear static analyses. Three material models are available in ABAQUS: concrete smeared cracking (SMS), brittle cracking (BC), and concrete damaged plasticity (CDP). In this study, the CDP model is used because it has been successfully applied in previous numerical studies for SFRC.[7,21]

The CDP model[22] uses a yield condition first developed by Lubliner et al.[23] and then modified by Lee and Fenves.[24] The ratio of biaxial to uniaxial compressive strength (σ_{b0}/σ_{c0}) and the ratio of the second stress invariant on the tensile meridian to that on the compressive meridian (K_C) are used in the CDP model to characterize the failure surface of concrete. The Drucker–Prager hyperbolic function is used in the CDP model to determine the flow potential. The dilation angle ψ and flow potential eccentricity ϵ are parameters used to define the flow rule. Since it was found that the addition of steel fibers does not significantly affect the Poisson's ratio ν for compressive strengths of less than 85 MPa,[25] a value of 0.2 was used in this study. Table 4 summarizes the values of the parameters used in the FE modeling for PC and HSFRC. The values were adopted following previous studies.[7,21,26]

The CDP model is coupled with the fictitious crack model[26] as an energy criterion, which is based on the fracture energy and is intended to prevent mesh sensitivity and allow numerical convergence. The behavior of concrete in tension can be described by a bilinear diagram (Figure 5) where the fracture energy, that is, the area under the diagram G_f, depends on the quality of the concrete and the aggregate size.[27] Due to the random orientation of the fibers in the concrete, it can be assumed that the tensile behavior of SFRC is similar to that of plain concrete, but with an improved tension stiffening.[28] The most common approach to determine the tensile characteristics is the inverse analysis, in which the tensile softening properties are gradually changed until the

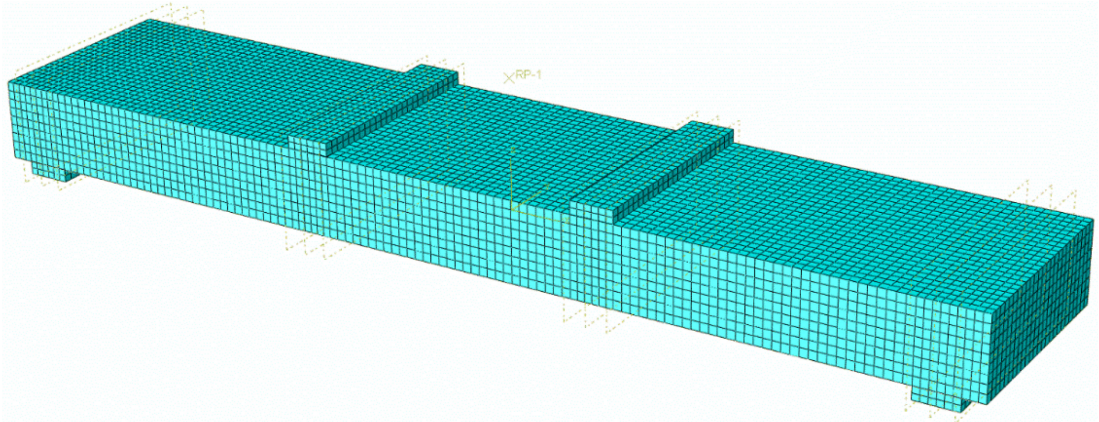

FIGURE 8 Geometry and mesh of slab model

TABLE 6 Concrete material properties

Mix	Compressive strength f_c (MPa)	Modulus of elasticity E (GPa)	Splitting tensile strength $f_{c,t}$ (MPa)	Flexural strength $f_{ct,L}$ (MPa)	Residual flexural strengths			
					$f_{R,1}$ (MPa)	$f_{R,2}$ (MPa)	$f_{R,3}$ (MPa)	$f_{R,4}$ (MPa)
PC	51.7 ± 0.1	33.91 ± 0.45	3.58 ± 0.32	4.64 ± 0.09	0.69 ± 0.14	0	0	0
HSFRC	51.9 ± 2.2	34.47 ± 0.82	6.13 ± 0.45	6.34 ± 0.39	7.54 ± 0.47	5.23 ± 0.41	3.90 ± 0.44	3.01 ± 0.44

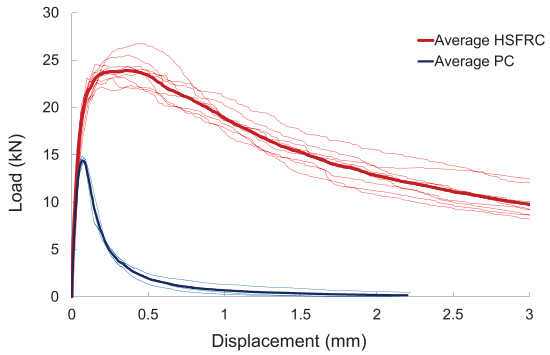

FIGURE 9 Load–displacement curves during flexural test

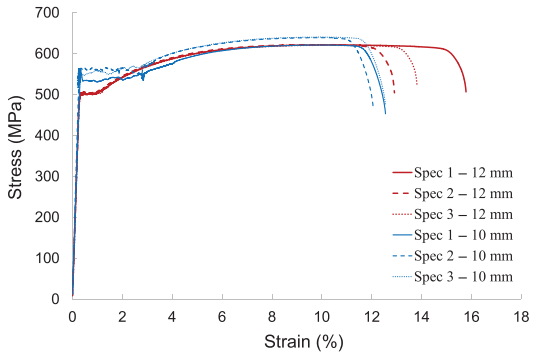

FIGURE 10 Reinforcing bar stress–strain curves

analytical load-deflection curve matches the experimental curve.

Previous studies have shown that for mixes with different types of fibers, a trilinear diagram can be used to show the behavior of concrete in tension.[29] The aim of this numerical test was to define a polylinear stress-crack opening law ($\sigma - w$) for the post-cracking behavior of a HSFRC mix reinforced with both manufactured steel fibers and recycled steel fibers. Figure 6 shows the developed material model of HSFRC. The parameters of the trilinear model that best fitted the experimental curves from the flexural test are summarized in Table 5. For the modulus of elasticity and tensile strength, the values obtained from laboratory tests were used.

TABLE 7 Mechanical properties of reinforcing steel

Property	Φ12 mm	Φ10 mm
Yield strength $R_{p0,2}$ (MPa)	505	540
Tensile strength R_M (MPa)	621	624
Total elongation A_t (%)	14.0	12.5
Elasticity module (GPa)	200	200

The adopted material model is validated using experimental results from notched prismatic specimens. The numerical model of a prismatic specimen with a length of 600 mm, a width of 150 mm, a height 150 mm, and a notch of 5 mm width and 25 mm length in the middle of

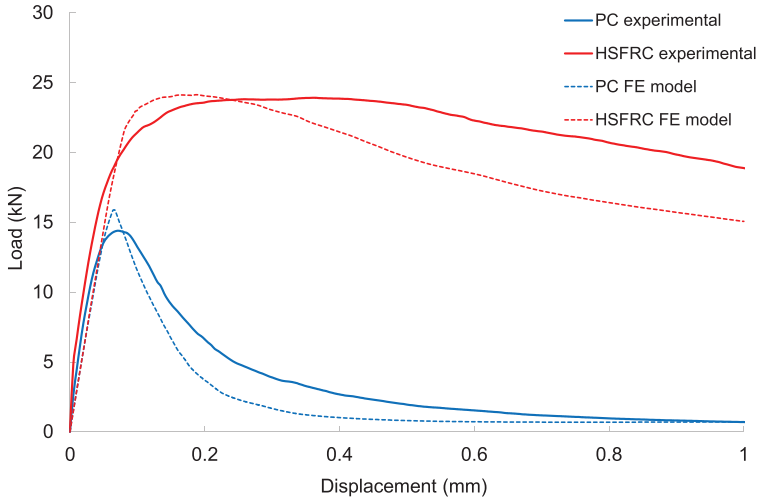

FIGURE 11 Validation of PC and HSFRC material model

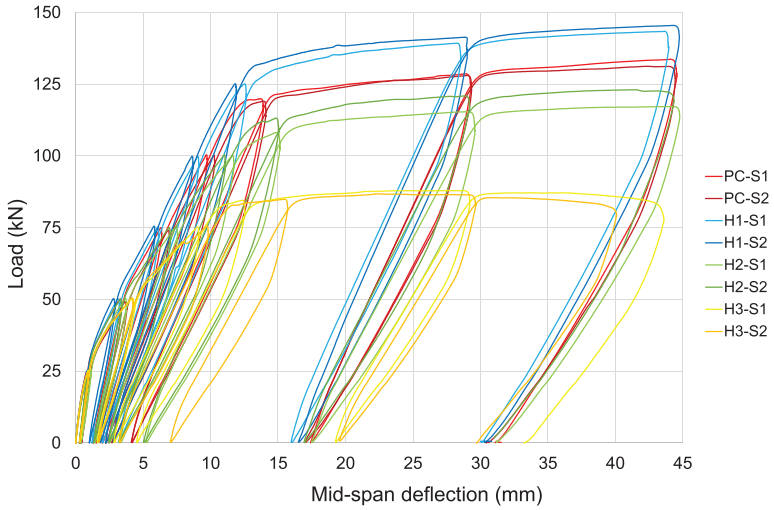

FIGURE 12 Load–mid-span deflection curves

the range is shown in Figure 7. An eight noded hexahedral elements were used for concrete with reduced integration (C3D8R). The same formulation was used to model the steel elements of the base and the press. The prism is based on steel bearings over contact surfaces for which a minimum coefficient of friction is defined.

After validating the material models, slab models with a length of 240 cm, a width of 50 cm, and a height of 18.5 cm were made. An eight noded hexahedral elements were used for concrete with reduced integration (C3D8R). The reinforcing bars were modeled as one-dimensional elements with two nodes (T3D2) embedded in the body of the block. The mesh of finite elements is formed so that they all have approximately the same size and regular shape. The length of the sides of the finite volume elements is 20 mm, Figure 8. The mesh adapts to the behavior of the concrete in the postcritical tension region, where the system is unstable and sensitive to the choice of mesh size. This is also the main problem of the FE method, since it is not possible to describe the discontinuous displacement function within the finite element.

4 | RESULTS AND DISCUSSION

4.1 | Material properties

Table 6 summarizes the average values of compressive strength, modulus of elasticity, splitting tensile strength, and residual flexural strength for each mix. The average results are given with standard deviations. The load–displacement curves for each specimen and the average curves are shown in Figure 9.

The results in Table 6 show that the addition of blended fibers has no effect on the compressive strength and modulus of elasticity. This was noted by others[30,31] who found that the low volume of fibers in the mix, as well as the nature of the failure, did not contribute to the properties described. However, others note[32] that an

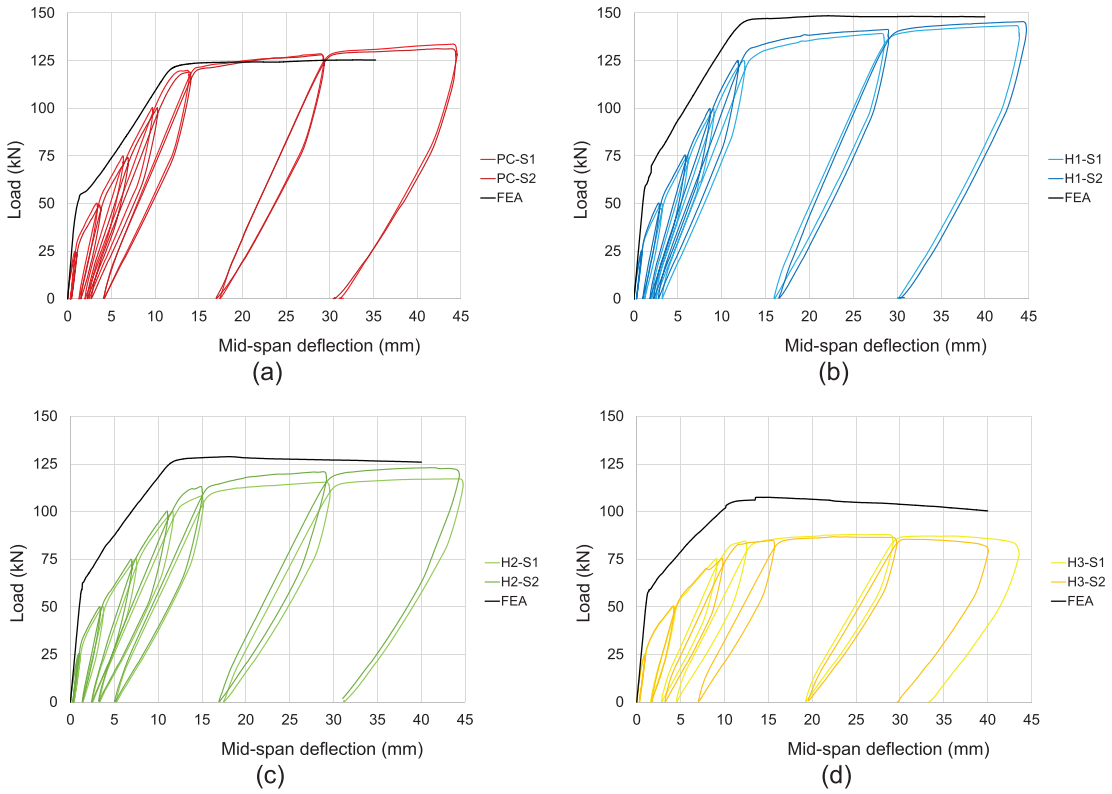

FIGURE 13 Experimental and numerical comparison of load-deflection curves for specimen types: (a) PC; (b) H1; (c) H2; and (d) H3

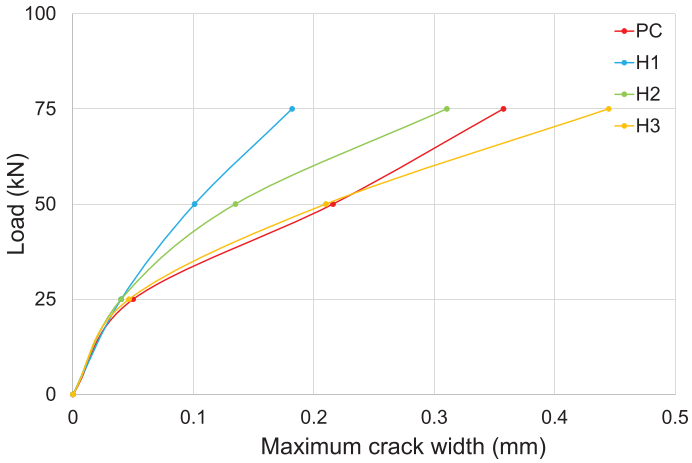

FIGURE 14 Load-maximum crack width curves

increase in compressive strength can be expected and is due to the ability of the steel fibers to control and delay microcrack coalescence and unstable crack propagation. When opposite trends are observed, the geometrical properties of the fibers used should always be considered as an important parameter influencing the described behavior.

The positive contribution of the fiber blend can be seen in the increase of the splitting tensile strength and the flexural strength. Both values increase by 1.7 and 1.4 times, respectively, for the HSFRC mixture compared to the plain concrete. This behavior was previously demonstrated for both MF and RTSF fibers and their combination.[9] It is due to the ability of the fibers to absorb energy after the first crack occurs, depending on the fiber geometry, with the length and diameter of the fibers having a significant effect on the toughness of the concrete.[33] The HSFRC, designed as an HSFRC mix, is based on fibers dimensions[34] and accounts for the fact that fibers with different geometries are activated at different fracture stages. Smaller fibers, in this case RTSF, bridge microcracks, control their growth, and retard coalescence, resulting in an increase in splitting and flexural strength. The second type of fiber is larger, in this case MF, and is used to stop the propagation of macrocracks. This leads to a significant improvement in the fracture toughness of the composite, which is reflected in the increase in residual flexural strength compared to plain concrete.

The properties of the reinforcing steel are shown in Figure 10 and Table 7.

4.2 | FE material model

The basic result of the numerical calculation is a diagram showing the relationship between the applied force acting on the reference point (press) and its displacement.

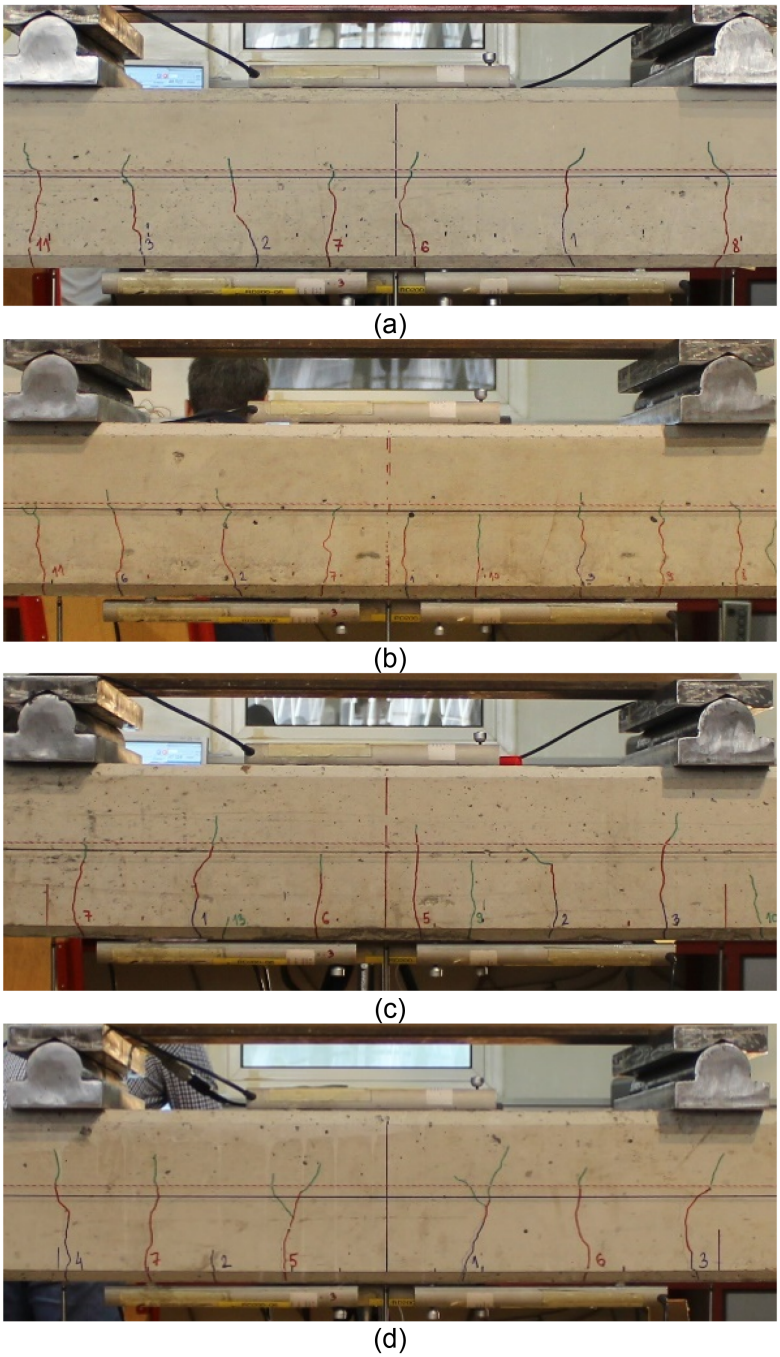

FIGURE 15 Cracking pattern in experimental test and numerical simulation at load F = 75 kN for specimens type (a) PC, (b) H1, (c) H2, and (d) H3

A comparison between the numerical simulation and the results of the experimental test on a notched prismatic specimens is shown in Figure 11. It can be seen that both numerical models describe the flexural behavior relatively well. The numerical models assume a slightly higher peak force, 2% for HSFRC and 10% for PC specimens, and a somewhat lower energy of absorption than the experimentally determined values, 12% for HSFRC, and 17% for PC specimens. The energy absorption capacity is the area under the load–displacement curve. Dividing it by the cross-section of the specimen gives the specific energy absorption capacity.[35] It is important to stress that presented model was developed for this hybrid steel fiber concrete mix. However, it can also simulate any other steel fiber content, provided that the model calibration is performed based on simple flexural tests on prismatic specimens.

4.3 | Real-scale specimens

The comparison of all measured properties was carried out at three load levels (25, 50, and 75 kN). The main interest of the research was to investigate the effects of

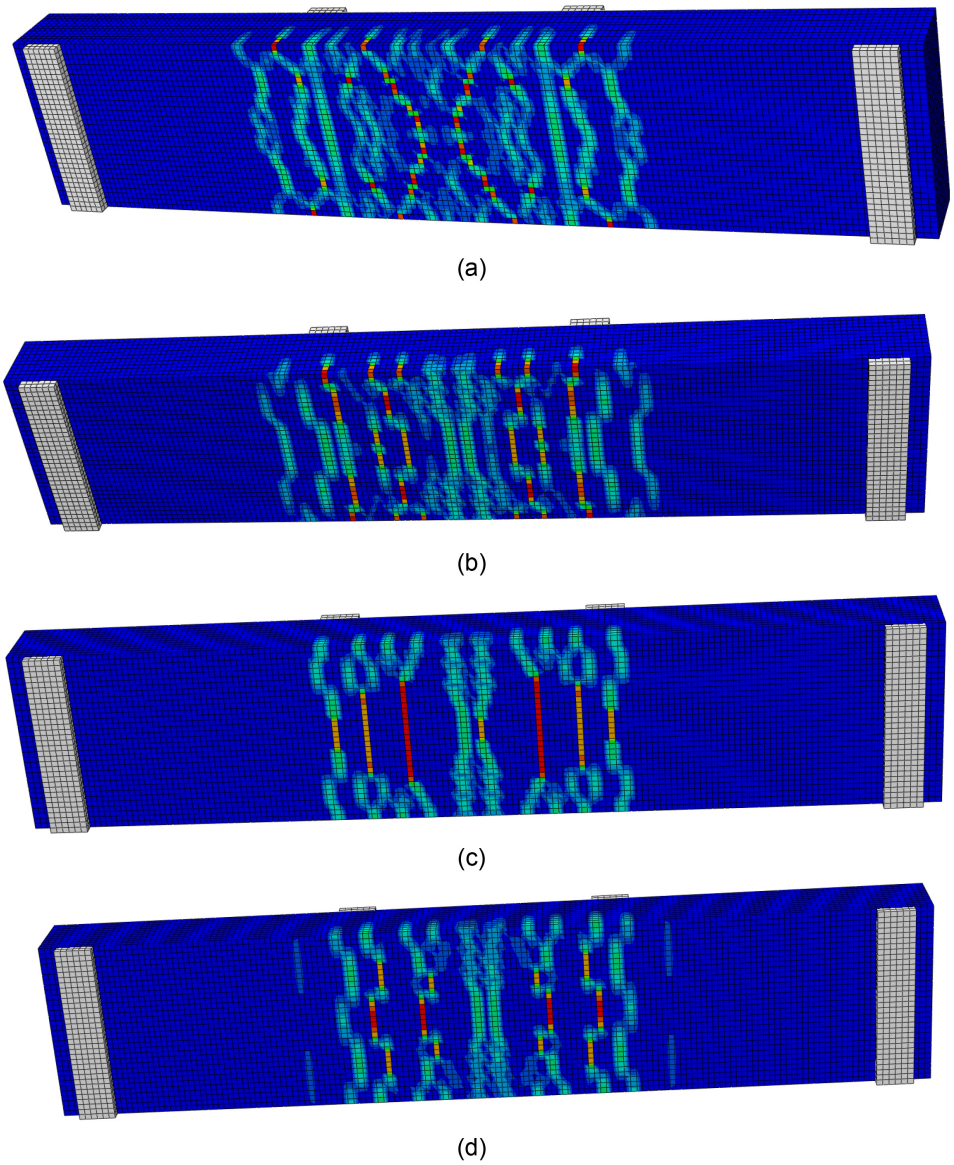

FIGURE 16 Cracking pattern in numerical simulation at load F = 75 kN for specimens type (a) PC, (b) H1, (c) H2, and (d) H3

the fibers on serviceability, as this is often the governing condition in designing bridge slab decks. *fib* model code[36] and *RILEM*[37] specify a maximum crack width of 0.3 mm as the serviceability limit for exposure class II. Therefore, the load level of 75 kN, where the reference PC specimens developed a crack of this width, was chosen as the serviceability limit.

Figure 12 shows the load–mid-span deflection curves for all tested specimens. The specimens developed a ductile flexural failure mode with significant yielding of the reinforcement. In general, the shape of the load–deflection curves is similar for all specimens. In each case, three sections with two changing points can be distinguished: the first crack and the yielding of the reinforcing steel. In the first section (until the first crack appeared), type H1 had a stiffness 2% higher than the reference type PC, 30.6 kN/mm compared to the reference 30 kN/mm. This means that the addition of fibers only slightly affects the elastic modulus of the concrete, which is consistent with the results of the material properties. Type H2 had the same stiffness as PC, indicating that the fibers compensate for the 20% reduction in reinforcement at this stage, while type H3 had 4% lower stiffness than the reference type PC. In the second section, after the first crack appears, the curves become flatter and the deflections increase in all cases. This was slower for the H1 series and faster for the H3 series, while the PC and H2 specimens behaved similarly. The benefit of the fibers resulted in an increase of yielding capacity. For the H1 series, the yield strength was 8% higher than for the PC series, reaching 131 kN (compared to 120 kN for PC), which is consistent with other studies.[38] This increase depends strongly on the ratio between the toughness and the reinforcement ratio.[38] For the H2

series, the yield strength was 8% lower than for the reference PC and 30% lower for the H3 series. The addition of fibers at this volume content was not sufficient to ensure the same behavior in ULS when conventional reinforcement is reduced. This is consistent with previous studies indicating that this is not the primary role of the fibers.[11]

Figure 13 shows a comparison of the experimental and numerical results in terms of load–mid-span deflection curves. The simulated response in terms of ultimate load and displacement is in good agreement with the experimental results. The numerical load-deflection response of all specimen types appears stiffer compared to the tested response. This may be due to possible initial pre-cracking before testing, for example, due to shrinkage or handling.[26] It must be mentioned that the complexity in the constitutive modeling of concrete and adoption of a perfect bond between concrete and reinforcement could also cause some deviations between numerical and experimental results.

The comparison of the maximum crack width over different loading levels is shown in Figure 14. The presence of the fibers throughout the concrete cross-section results in better control of cracking because they act over the entire tensile block, unlike a conventional concrete. The maximum crack widths are reduced by 20%–53% for type H1. These results are in line with those of Gholamhoseini et al.,[13] who reported that the addition of 60 kg/m^3 fibers can reduce the maximum crack width by up to 50%. The maximum crack widths are reduced by 13%–38% for type H2, while type H3 behaves similarly to the reference type PC. It was observed that slightly more cracks opened with smaller widths and at smaller distances from each other in slab types H1 and H2 compared to slabs of type PC, while slabs of type H3 behaved similarly to slabs of plain concrete, Figure 15.

The maximum tensile principal stresses can be used in FEA to show the crack patterns. However, the maximum plastic equivalent principal strains give a better representation of the cracking. For this reason, the strains are used to represent the crack patterns. The crack pattern for each specimen type at load level F = 75 kN is shown in Figure 16. The crack patterns determined in the FEA are similar to those obtained by experiment.

5 | CONCLUSION

This paper presents an experimental and numerical study on the potential application of a hybrid mixture of manufactured and recycled steel fibers from waste car tyres to reinforced concrete elements. Eight slab specimens with different reinforcement ratios were subjected to a four-point bending test to measure displacements, crack widths and to investigate the possibility of partially replacing the conventional reinforcement with steel fibers. The results are mainly focused on service level performance. The greatest contribution was observed in the control of crack propagation. The addition of a hybrid fiber mix to a conventionally reinforced concrete slab (type H1) significantly reduced crack widths (up to 53%). The addition of fibers compensated for a conventional reinforcement reduction of 20% (type H2) by reducing crack widths by up to 38%. Type H3 with 44% reinforcement reduction behaved similarly to the reference type PC. Overall, it can be concluded that by adding this hybrid fiber blend in concrete elements, a reduction of reinforcement by 20% can be achieved with better behavior in terms of serviceability limit criterion.

Using numerical models in Abaqus simulating the flexural test on notched prismatic specimens, a calibration of the material models of plain concrete and HSFRC was performed based on the test results. These validated material models were used for numerical modeling of slabs and the results were compared with the experimental values in terms of deflection, strength, and crack pattern. The results of the analyses compared to the test results showed good agreement. The FEA results confirm the ability of the proposed HSFRC material model to predict the flexural behavior of slabs with conventional reinforcement. The presented analyses indicate that the proposed model can be used in future parametric studies on various aspects of concrete slabs in flexure.

ACKNOWLEDGMENTS

The authors wish to acknowledge the financial support of the 7th Framework Programme of the European Community "Innovative Use of All Tyre Components in Concrete" under contract number 603722. The authors gratefully acknowledge all the participants in the above mentioned project with special thanks to colleagues from Faculty of Civil Engineering Zagreb, Department of Engineering Mechanics and Department of Materials.

DATA AVAILABILITY STATEMENT

The data that support the findings of this study are available on request from the corresponding author. The data are not publicly available due to privacy or ethical restrictions.

ORCID

Marina Frančić Smrkić https://orcid.org/0000-0001-5346-6961

REFERENCES

1. Baricevic A, Bjegovic D, Skazlic M. Hybrid fiber-reinforced concrete with unsorted recycled-tire steel fibers. J Mater Civ

Eng. 2017;29(6):06017005. https://doi.org/10.1061/(asce)mt.1943-5533.0001906
2. Graeff AG, Pilakoutas K, Neocleous K, Peres MVNN. Fatigue resistance and cracking mechanism of concrete pavements reinforced with recycled steel fibres recovered from post-consumer tyres. Eng Struct. 2012;45:385–95. https://doi.org/10.1016/j.engstruct.2012.06.030
3. Tlemat H, Pilakoutas K, Neocleous K. Stress–strain characteristic of SFRC using recycled fibres. Mater Struct. 2006;39:365–77. https://doi.org/10.1617/s11527-005-9009-4
4. Neocleous K, Tlemat H, Pilakoutas K. Design issues for concrete reinforced with steel fibers, including fibers recovered from used tires. J Mater Civ Eng. 2006;18(5):677–85.
5. Ahmed HU, Faraj RH, Hilal N, Mohammed AA, Sherwani AFH. Use of recycled fibers in concrete composites: a systematic comprehensive review. Compos Part B Eng. 2021;215:108769. https://doi.org/10.1016/j.compositesb.2021.108769
6. Hu H, Papastergiou P, Angelakopoulos H, Guadagnini M, Pilakoutas K. Mechanical properties of SFRC using blended manufactured and recycled tyre steel fibres. Construct Build Mater. 2018;163:376–89. https://doi.org/10.1016/j.conbuildmat.2017.12.116
7. Hu H, Wang Z, Figueiredo FP, Papastergiou P, Guadagnini M, Pilakoutas K. Postcracking tensile behavior of blended steel fiber-reinforced concrete. Struct Concr. 2019;20(2):707–19. https://doi.org/10.1002/suco.201800100
8. Bartolac M. Properties of precast constructive elements with reinforcement partially replaced with recycled steel fibres. Zagreb, Croatia: University of Zagreb; 2015.
9. Frančić Smrkić M, Damjanović D, Baričević A. Application of recycled steel fibres in concrete elements subjected to fatigue loading. Gradjevinar. 2017;69(10):893–905. https://doi.org/10.14256/JCE.2059.2017
10. Zollo RF. Fiber-reinforced concrete: an overview after 30 years of development. Cem Concr Compos. 1997;19(2):107–22. https://doi.org/10.1016/S0958-9465(96)00046-7
11. Groli G, Caldentey AP. Improving cracking behaviour with recycled steel fibres targeting specific applications––analysis according to *fib* model code 2010. Struct Concr. 2017;18(1):29–39. https://doi.org/10.1002/suco.201500170
12. Vandewalle L. Mechanical and cracking behavior of concrete beams reinforced with steel bars and short fibers. Mater Struct Constr. 2000;33(April):164–70.
13. Gholamhoseini A, Khanlou A, MacRae G, Scott A, Hicks S, Leon R. An experimental study on strength and serviceability of reinforced and steel fibre reinforced concrete (SFRC) continuous composite slabs. Eng Struct. 2016;114:171–80. https://doi.org/10.1016/j.engstruct.2016.02.010
14. McMahon JA, Birely AC. Service performance of steel fiber reinforced concrete (SFRC) slabs. Eng Struct. 2018;168(April):58–68. https://doi.org/10.1016/j.engstruct.2018.04.067
15. EN 12390-3. Testing Hardened Concrete––Part 3: Compressive Strength of Test Specimens; 2012.
16. EN 12390-6. Testing Hardened Concrete. Determination of Secant Modulus of Elasticity in Compression; 2013.
17. EN 12390-6. Testing Hardened Concrete––Part 6: Tensile Splitting Strength of Test Specimens; 2010.
18. EN 14651. Test Method for Metallic Fibre Concrete–Measuring the Flexural Tensile Strength; 2008.
19. EN ISO 15630-1. Steel for the Reinforcement and Prestressing of Concrete––Test Methods Part 1: Reinforcing Bars, Rods and Wire; 2019.
20. EN ISO 6892-1. Metallic Materials––Tensile Testing Part 1: Method of Test at Room Temperature; 2019.
21. An C, Castello X, Duan M, Toledo Filho RD, Estefen SF. Ultimate strength behaviour of sandwich pipes filled with steel fiber reinforced concrete. Ocean Eng. 2012;55:125–35. https://doi.org/10.1016/j.oceaneng.2012.07.033
22. Abaqus User's Manual. 2017:1–14.
23. Lubliner J, Oliver J, Oller S, Onate E. A plastic-damage model. Int J Solids Struct. 1989;25(3):299–326.
24. Lee J, Fenves GL. Plastic-damage model for cyclic loading of concrete structures. J Eng Mech. 1998;124(8):892–900. https://doi.org/10.1061/(asce)0733-9399(1998)124:8(892)
25. Swaddiwudhipong S, Seow PEC. Modelling of steel fiber-reinforced concrete under multi-axial loads. Cem Concr Res. 2006;36(7):1354–61. https://doi.org/10.1016/j.cemconres.2006.03.008
26. Genikomsou AS, Polak MA. Finite element analysis of punching shear of concrete slabs using damaged plasticity model in ABAQUS. Eng Struct. 2015;98:38–48. https://doi.org/10.1016/j.engstruct.2015.04.016
27. Shewalul YW. Numerical and FEA investigation of sectional capacity and moment redistribution behavior of steel fiber reinforced concrete (SFRC) beam. Heliyon. 2021;7(6):e07354. https://doi.org/10.1016/j.heliyon.2021.e07354
28. Tlemat H, Pilakoutas K, Neocleous K. Modelling of SFRC using inverse finite element analysis. Mater Struct. 2006;39(May):221–33. https://doi.org/10.1617/s11527-005-9009-4
29. Sorelli LG, Meda A, Plizzari GA. Bending and uniaxial tensile tests on concrete reinforced with hybrid steel fibers. J Mater Civ Eng. 2005;17(5):519–27. https://doi.org/10.1061/(asce)0899-1561(2005)17:5(519)
30. Centonze G, Leone M, Aiello MA. Steel fibers from waste tires as reinforcement in concrete: a mechanical characterization. Construct Build Mater. 2012;36:46–57. https://doi.org/10.1016/j.conbuildmat.2012.04.088
31. Martinelli E, Caggiano A, Xargay H. An experimental study on the post-cracking behaviour of hybrid industrial/recycled steel fibre-reinforced concrete. Construct Build Mater. 2015;94:290–8. https://doi.org/10.1016/j.conbuildmat.2015.07.007
32. Alsaif A, Garcia R, Figueiredo FP, Neocleous K, Christofe A, Guadagnini M, et al. Fatigue performance of flexible steel fibre reinforced rubberised concrete pavements. Eng Struct. 2019;193:170–83. https://doi.org/10.1016/j.engstruct.2019.05.040
33. Markovic I. High-performance hybrid-fibre concrete: development and utilisation. Delft, Netherlands: Delft University Press; 2006.
34. Banthia N, Gupta R. Hybrid fiber reinforced concrete (HyFRC): fiber synergy in high strength matrices. Mater Struct Constr. 2004;37(274):707–16. https://doi.org/10.1617/14095
35. Poletanovic B, Dragas J, Ignjatovic I, Komljenovic M, Merta I. Physical and mechanical properties of hemp fibre reinforced alkali-activated fly ash and fly ash/slag mortars. Construct Build Mater. 2020;259:119677. https://doi.org/10.1016/j.conbuildmat.2020.119677
36. du Beton FI. *Fib* model code for concrete structures. Berlin, Germany: Wilhelm Ernst & Sohn; 2010.

37. RILEM. Final Recommendation F. RILEM TC 162-TDF: "Test and design methods for steel fibre reinforced concrete" σ-ε-design method. Mater Struct Constr 2003;36(262):560–567. doi:https://doi.org/10.1617/14007
38. Meda A, Minelli F, Plizzari GA. Flexural behaviour of RC beams in fibre reinforced concrete. Compos Part B Eng. 2012;43(8):2930–7. https://doi.org/10.1016/j.compositesb.2012.06.003

AUTHOR BIOGRAPHIES

Marina Frančić Smrkić, Department of Engineering Mechanics, Faculty of Civil Engineering, University of Zagreb, Zagreb, Croatia. Email: marina.francic.smrkic@grad.unizg.hr.

Domagoj Damjanović, Department of Engineering Mechanics, Faculty of Civil Engineering, University of Zagreb, Zagreb, Croatia. Email: domagoj.damjanovic@grad.unizg.hr.

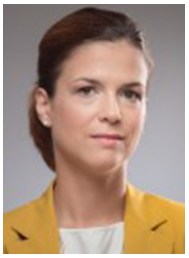

Ana Baričević, Department of Materials, Faculty of Civil Engineering, University of Zagreb, Zagreb, Croatia. Email: ana.baricevic@grad.unizg.hr.

Mario Uroš, Department of Engineering Mechanics, Faculty of Civil Engineering, University of Zagreb, Zagreb, Croatia. Email: mario.uros@grad.unizg.hr.

How to cite this article: Frančić Smrkić M, Damjanović D, Baričević A, Uroš M. Experimental and numerical analysis of concrete slabs reinforced with rebar and recycled steel fibers from waste car tyres. Structural Concrete. 2023;24(2):1807–20. https://doi.org/10.1002/suco.202200640